Articles

Imaging and Mapping Heparin-Binding Sites on Single Fibronectin Molecules with Atomic Force Microscopy†

Hai Lin,*,‡,§ Ratnesh Lal,‡ and Dennis O. Clegg‡,§

Neuroscience Research Institute and Department of Molecular, Cellular, and Developmental Biology, University of California, Santa Barbara, California 93106

Received July 14, 1999; Revised Manuscript Received November 10, 1999

ABSTRACT: Fibronectin is composed of multiple homologous repeats and contains many functional domains. Two major heparin-binding domains have previously been identified: the Hep I site near the amino terminus and the Hep II site near the carboxyl terminus. The Hep II site has been considered the high-affinity heparin-binding site based on studies of fibronectin fragments. However, few studies have been carried out on heparin binding by intact fibronectin. We imaged single fibronectin molecules as well as heparin-coated gold particles bound to whole dimeric plasma fibronectin molecules with tapping mode atomic force microscopy. We observed heparin−gold particles preferentially bound at two locations that correspond to the Hep I and Hep II sites. Quantitative analysis of images of individual fibronectin−heparin−gold complexes showed that almost twice as many heparin−gold particles bound to the N-terminal Hep I site compared to the Hep II site. In contrast to previous findings with fibronectin fragments, these results suggest that the Hep I site has a binding affinity higher than or comparable to the Hep II site in the intact fibronectin molecule.

Fibronectin (Fn)[1] is an adhesive glycoprotein that has been shown to play major roles in development, wound healing, immune responses, and tumor metastasis (*1*−*3*). It is an abundant component of the extracellular matrix, blood plasma, and other body fluids. Fn is a dimeric molecule, composed of two very similar monomers joined near their carboxyl terminus by two disulfide bonds. Each Fn monomer consists of many repeating domains designated as type I, type II, and type III repeats (see Figure 1). These repeating structures contain multiple functional domains which bind to other extracellular matrix molecules, glycosaminoglycans and proteoglycans, bacteria, viruses, and cells via multiple surface receptors (*2, 3*). The principle cell-binding region is centered around the sequence Arg-Gly-Asp (RGD) and has been shown to interact with cell integrin receptors $\alpha_5\beta_1$ and $\alpha_v\beta_1$ (*4, 5*). Some cells also interact with LDV and REDV motifs in the alternatively spliced V (CS-1) domain via the $\alpha_4\beta_1$ and $\alpha_4\beta_7$ integrins (*6*). After the attachment of cells to the Fn cell-binding domain, a heparin-binding activity is required for formation of focal adhesions (*7, 8*).

Fibronectin binds to heparin (*9, 10*), and studies using whole Fn molecules suggested that Fn contains at least two distinct heparin-binding sites with different affinities (*9, 11*). Utilizing enzymatically digested Fn fragments, at least three heparin-binding sites have been mapped to specific regions of Fn (*3, 9, 12*−*20*). Two of the heparin-binding sites, named Hep I and Hep II, are considered most physiologically relevant. Hep I and Hep II are located at opposite ends of the monomeric fibronectin, near the amino and carboxyl termini, respectively (Figure 1). Both Hep I and Hep II promote cell adhesion and attachment independent of integrin receptors (*21*−*23*). In addition, Hep II also binds integrin $\alpha_{IIb}\beta_3$ in a RGD-independent manner (*24*). Both heparin-binding sites are crucial for Fn fibrillogenesis and extracellular matrix formation (*25*−*28*). Hep II is thought to have the highest affinity for heparin (*3, 14, 18, 19*). One study using Fn fragments suggested that the Hep II binding affinity could be up to 100-fold higher than that of Hep I (*18*). Studies using protein fragments, synthetic peptides, and site-specific mutagenesis suggest that binding of Fn to heparin and to the cell surface via Hep I and Hep II involves multiple and discontinuous sites (*29, 30*). A recent study even uncovered a cryptic anti-adhesive structure within the Hep II domain (*31*). However, few studies have addressed heparin-binding sites and affinities by the intact Fn molecule.

We have examined interactions between heparin and whole Fn molecules using atomic force microscopy (AFM). This method allows real-time and high-resolution imaging of biological specimens ranging from single molecules to whole

† This work was supported by NIH Grants EY09736 (H.L.), GM056290 (R.L.), and EY066570 (D.O.C.) and by grants from Santa Barbara Cottage Hospital.

* To whom correspondence should be addressed at the Neuroscience Research Institute, University of California, Santa Barbara, CA 93106. E-mail: h_lin@lifesci.ucsb.edu; FAX: 805-893-2005; TEL: 805-893-8490.

‡ Neuroscience Research Institute.

§ Department of Molecular, Cellular, and Developmental Biology.

[1] Abbreviations: Fn, fibronectin; AFM, atomic force microscopy; PBS, phosphate-buffered saline.

10.1021/bi991624o CCC: $19.00
Published on Web 02/29/2000

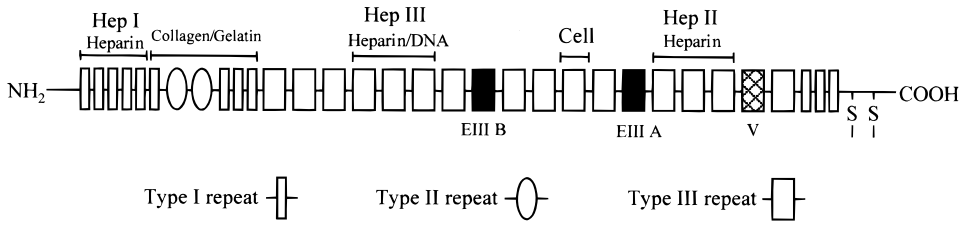

FIGURE 1: Schematic representation of the primary sequence and selected functional domains of monomeric fibronectin. The protein is composed of a series of homologous repeats of types I, II, and III. The three heparin-binding domains are shown at the top. Hep I encompasses the first 5 type I repeats near the N-terminus, and Hep II has been localized to the 12th, 13th, and 14th type III repeats. The cell-binding (RGD) domain is located at the 10th type III repeat. Domains EIIIA, EIIIB, and V, which may be spliced in or out during RNA processing, are also shown.

cells and tissues (*32*). AFM has been used to examine various physical and biochemical interactions between macromolecules, such as receptor−ligand and antibody−antigen interactions (*33*, *34*). Recently, AFM was used to image the binding of human factor IX to collagen IV at specific sites (*35*) and the real-time proteolysis of single collagen I molecules (*36*). In the present study, we imaged binding of heparin-coated colloidal gold particles to single fibronectin molecules and quantified their distribution. Surprisingly, our results suggest that the Hep I site has an affinity higher than or comparable to the heparin-binding affinity of the Hep II site.

EXPERIMENTAL PROCEDURES

Sample Preparation. Bovine plasma Fn (1 mg/mL) was purchased from Life Technologies, Inc. (Rockville, MD); colloidal gold particles (5 nm diameter) absorbed with heparin−albumin were purchased from Sigma Chemical Co. (St. Louis, MO); and colloidal gold particles (6 nm diameter) absorbed with bovine albumin were purchased from Electron Microscopy Sciences (Ft. Washington, PA). For imaging uncoupled single Fn molecules, Fn was diluted to 1 μg/mL in phosphate-buffered saline (PBS, Life Technologies, Inc.) containing 1 mM Ca^{2+} and 1 mM Mg^{2+}. Diluted Fn was absorbed to a freshly cleaved mica surface and incubated at room temperature for 1−2 min. The mica was then thoroughly rinsed with deionized water, and compressed argon gas was used to remove water from the mica surface and dry the sample.

To analyze Fn interactions with heparin, 2−5 μg of Fn ($\sim 1 \times 10^{13}$ molecules) was incubated with 1 μL of heparin−albumin-coated gold particles and albumin-coated gold particles ($\sim 2 \times 10^{11}$ particles, 2×10^{14} mL^{-1}; particle diameter ~3.5−6.5 nm) in 0.2 mL of PBS containing 1 mM Ca^{2+} and 1 mM Mg^{2+} for 2−12 h at 4 °C. Glutaraldehyde was then added to a final concentration of 0.1%, and the solution was further incubated for 30 min. We empirically chose a significantly higher Fn concentration compared to heparin−gold particles to ensure that most heparin−albumin−gold particles are coupled to a Fn molecule.

Two different methods were used to separate coupled Fn−heparin−gold complexes from uncoupled Fn molecules: (1) The mixture was diluted with PBS and centrifuged at 10000*g* to pellet Fn−heparin−gold complexes, and the supernatant was discarded. This procedure was repeated at least 3 times for each sample preparation. (2) The Fn−heparin−gold complexes were separated from uncoupled Fn by size-exclusion chromatography. After glutaraldehyde fixation, the Fn−heparin−gold mixture was chromatographed on a Sephacryl S-500 column (6−10 mL volume, Pharmacia) in PBS. Fractions (0.25 mL) were collected, and the content of gold particles in each fraction was determined by optical absorption at 520 nm using a Beckman DU 640B spectrophotometer. Generally, the fraction containing the highest gold particle concentration was used for atomic force microscopy imaging.

Atomic Force Microscopy. For atomic force microscopy imaging, samples were absorbed on freshly cleaved mica for 2 min in PBS, rinsed with deionized water, and dried with compressed argon gas. The atomic force microscope used in this study was a Nanoscope III Multimode with an Extender electronics module for phase imaging (Digital Instruments, Santa Barbara, CA). All samples were imaged in tapping mode, in air, using a D scanner (maximum scan size $\approx$ 11 μm) and Tapping Mode etched silicon probes (125 μm in length, spring constant ~2−10 N/m, resonance frequency ~200−400 kHz, tip oscillation amplitude ~10−20 nm). The scan rates were between 3 and 15 Hz, and the proportional and integral gains were set between 0.2 and 0.6. Both height and phase images of the samples were recorded. Images presented in the paper are flattened, and some are zoomed and low-pass-filtered using the Digital Instruments Nanoscope III software program.

RESULTS

Fn is a dimer, formed by two very similar monomers which are joined near their C-termini by two disulfide bonds. Figure 2A shows a typical image of single bovine plasma Fn molecules absorbed on mica. Most of the imaged Fn molecules were in a partially extended, V-shaped form (Figure 2B−D) and exhibited folded domains on their extended arms. The lengths of these extended Fn molecules ranged between 120 and 160 nm, with each extended arm of the V ranging between 60 and 80 nm under lower resolution imaging. The height of the Fn molecules was about 1 nm. These images are consistent with the known structure of Fn and are similar to previous electron microscopy images (*37*, *38*). High-resolution AFM images also show the foldings of Fn peptide backbone (Figure 2D). After fixation with 0.1% glutaraldehyde and size-exclusion chromatography (see Experimental Procedures), the appearance of single Fn molecules was basically unchanged.

The heparin−albumin-absorbed colloidal gold particles were imaged on mica in the absence of Fn (Figure 2E). The height of the imaged gold particles varied between 3 and 6 nm, consistent with the manufacturer's specifications. The width of the imaged gold particles ranged between 8 and 20 nm, due to the broadening effect of the tip.

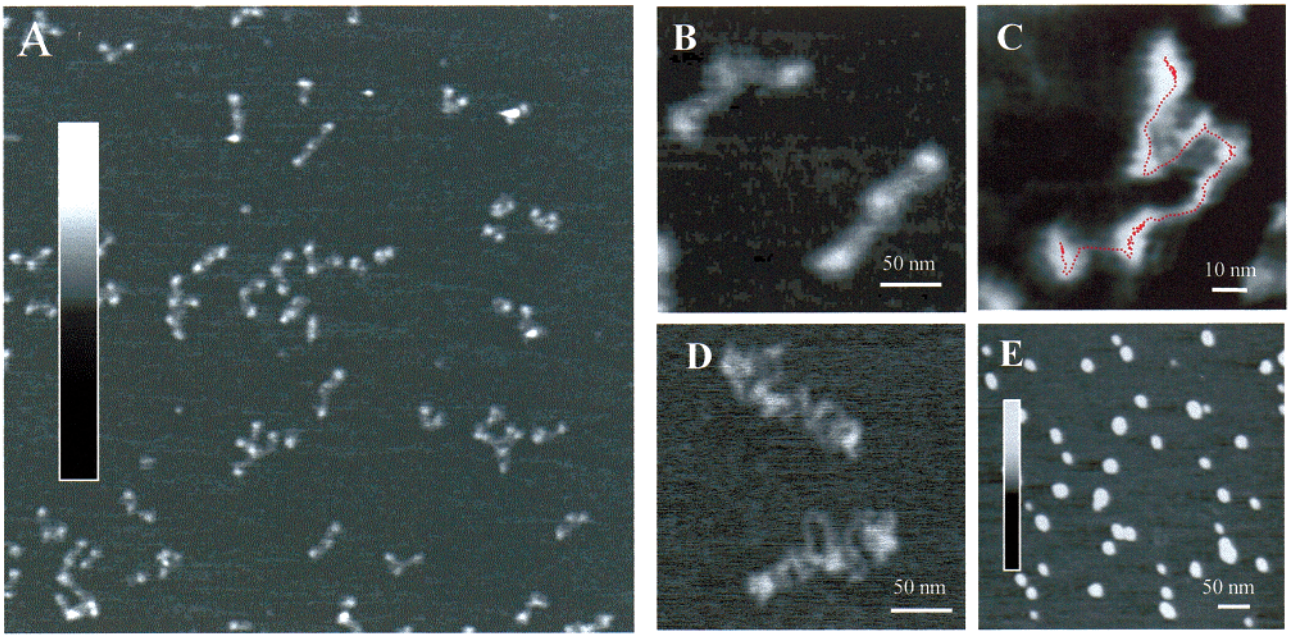

FIGURE 2: Height mode atomic force microscope images of Fn molecules and heparin−gold particles on mica. (A) A typical unprocessed, scanned image of Fn molecules on mica, scan size 1.6 μm × 1.6 μm. (B) Unprocessed images of individual Fn molecules. (C) A single Fn molecule with an extended arm and a partially folded arm; the peptide backbones of the Fn dimers are indicated by dotted lines. (D) Unprocessed high-resolution image of two dimeric Fn molecules, which shows the folding of the Fn peptide backbones. (E) Unprocessed height mode image of 5 nm diameter heparin−albumin−gold particles. The height is gray-scale-coded from 0 (black) to 3 nm (white) for panels A−D and 0−10 nm for panel E.

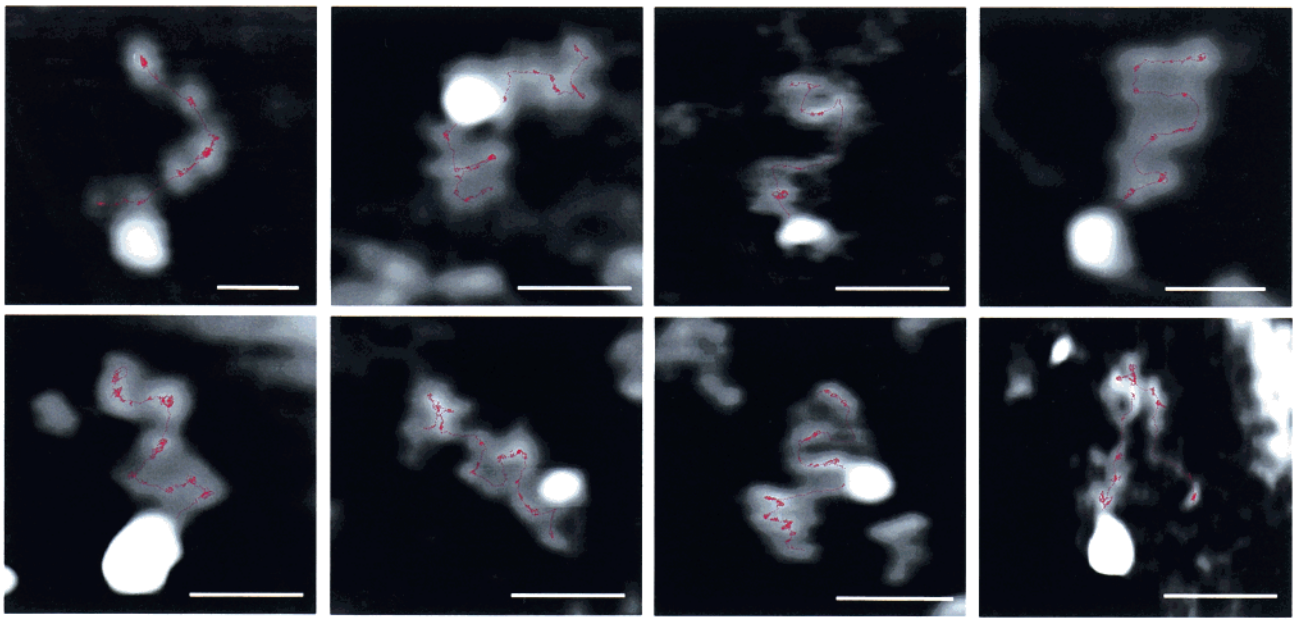

FIGURE 3: Representative height mode images of heparin−gold particles bound to Fn molecules. The inferred peptide backbone of the Fn dimer is indicated by a dotted line. Scale bars: 50 nm.

Representative images of a single heparin−albumin−gold particle bound to an individual Fn molecule are shown in Figure 3. We did not observe binding between Fn and gold particle coated only with albumin (data not shown), indicating that binding of heparin−albumin−gold particles to Fn was not due to the nonspecific effect of glutaraldehyde fixation. Because the heparin−gold particles have a greater height than Fn, they appeared as brighter spots than Fn, which appeared as gray in the height mode images. In some cases, it was difficult to image Fn in the height mode, so we also used phase mode imaging, which detects differences in stiffness of the sample (Young's module) and energy dissipation of sample−tip interactions (*39, 40*). In cases where heparin−gold particles can be clearly localized on the Fn dimer, the heparin−gold particle binding sites predominantly fell either in or near the center of the Fn dimer (corresponding to the C-termini of Fn monomers) or at or near one of the N-termini.

We randomly sampled 103 heparin−gold/Fn-binding events where the binding location on Fn could be clearly defined (Figure 4). In plotting the data, the Fn N-terminus closest to the heparin−gold particle was defined as the starting point (0 nm on the *x*-axis). Heparin−gold particles mostly bound at two locations on Fn. A major peak was

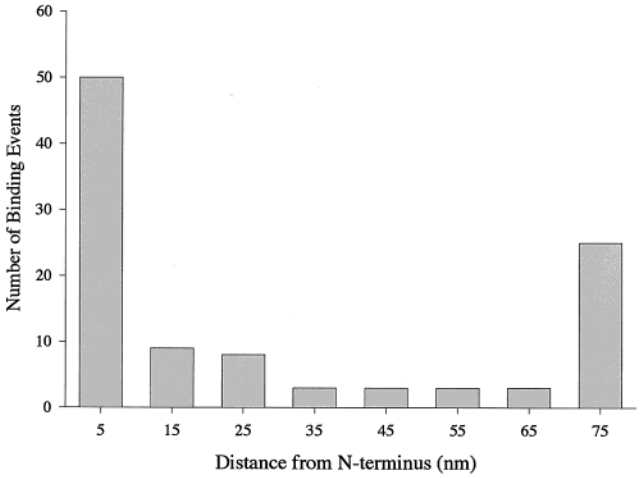

FIGURE 4: Distribution of heparin−gold particle binding events on single dimeric Fn molecules in 10 nm increments. The origin of the *x*-axis was defined as the Fn N-terminus closest to the gold particle. The center of the Fn dimer (corresponding to the C-terminus of the Fn monomer) is approximately 70 nm from the N-terminus.

localized to the N-terminus, and a minor peak was located near the center of the dimeric molecule (near the C-terminus of the Fn monomer). Approximately twice as many heparin−gold particles were mapped to the N-terminal site. Both peaks are statistically significant ($P < 0.001$, Student's *t* test).

DISCUSSION

In the present study, we have imaged single Fn molecules and the binding of heparin−gold particles to single Fn molecules using tapping mode atomic force microscopy with height and phase imaging. These results enabled us to map the heparin-binding sites to specific regions of the Fn molecule and analyze the relative binding affinity of the two sites. Our results suggest that the Hep I domain has a binding affinity higher than or comparable to that of the Hep II domain.

Most of the imaged Fn molecules are in relatively extended form, many with some partial folding at one or both N-termini (Figure 3). Previous EM and biophysical studies have suggested that Fn molecules are folded in low salt solutions (2 mM) and are extended in higher salt (0.2 M) and high pH buffers (*41, 42*). In the present study, Fn was absorbed to mica in a physiological buffer (PBS) and washed with deionized water before drying. Under such conditions, imaged plasma Fn molecules should either maintain their physiological conformation or assume the more folded form under the low salt conditions of the wash. Thus, the more abundant extended form of Fn is likely to resemble its conformation in physiological conditions. While, we cannot rule out the possibility that absorption of Fn to the mica surface may alter its conformation, the heparin particles were bound to Fn in physiological buffer and cross-linked before analysis by AFM.

Fibronectin contains at least three known heparin-binding sites, Hep I, II, and III. Among the three heparin-binding sites, the C-terminal Hep II site is generally considered to have the highest affinity for heparin, and the N-terminal Hep I site is often referred to as the intermediate-affinity heparin-binding site (*3, 14, 18, 19*). In our present study, about 50% of the heparin-binding events occurred at or near the amino terminus of Fn, around the Hep I site; only about half as many binding events occurred around the C-termini of the monomers, corresponding to the Hep II site (Figure 4).

There could, however, be several sources of error which might affect the data summarized in Figure 4: (1) Tracing the contour length of Fn was done manually using the Nanoscope III software, which could have introduced slight systematic errors in estimating the lengths of Fn molecules and relative heparin-binding locations; (2) assigning heparin−gold binding locations on Fn molecules could have also introduced uncertainty, since a heparin−gold particle could bind slightly more to the left or right of where binding was assumed to have occurred; (3) only binding events where the location could clearly be defined were counted, which could also have introduced uncertainty. However, all of these possible errors and uncertainties would not have significantly altered the basic result summarized in Figure 4: for intact plasma Fn, the N-terminal Hep I region contains a high-affinity binding site for heparin, and this affinity is comparable if not higher than that of the Hep II region.

Nearly all previous studies of heparin−Fn interactions have employed different proteolytic Fn fragments (*12*−*20, 29*). The major heparin-binding activity of the Hep II site has been localized to the 13th type III repeat, with additional contributions from the 12th and 14th type III repeats. Heparin binding to the Hep II region is likely to be very dependent on the three-dimensional structure of the Fn molecule. A recent structural study indicated that heparin binding by the type III 13th repeat alone involves six discontinuous amino acid sequences and these remote sequences fold together to form a "cation cradle" which binds heparin (*29*). A study by Siri et al. (*17*) showed that a larger Fn fragment (145−155 kDa) containing the Hep II region had lower heparin-binding affinity than the smaller 29/38 kDa Hep II fragment, which suggests that the Hep II domain may be cryptic and masked by other regions of the protein. Thus, fragmentation of Fn molecules, which may alter the tertiary structure of the heparin-binding domains, could affect the heparin-binding affinity of these domains. Other such cryptic sites have been identified in laminin-1, where an RGD adhesive site is exposed only after proteolysis in vitro (*43*).

Interestingly, one of the earliest studies of Fn heparin-binding domains and binding affinity used whole Fn molecules instead of predigested fragments (*10*). In that study, intact cellular Fn molecules were allowed to bind to heparin−agarose affinity columns, then digested in situ with α-chymotrypsin and Pronase. After proteolysis and an extensive wash, the proteolytic Fn fragment that remained bound to the heparin column was a 50 kDa terminal fragment, which includes the Hep I but not the Hep II region. These results are consistent with our study and suggest that the N-terminal Hep I region is the higher affinity heparin-binding domain in intact Fn.

Assembly of Fn into an extracellular matrix involves multiple domains and multiple consecutive binding interactions between Fn and integrins, Fn itself, and other extracellular matrix molecules such as collagen I (*44, 45*). Interactions with heparin are critical for self-assembly of Fn into fibrils (*11*). Self-assembly of Fn has been shown to require the Hep I and Hep II domains, as well as the first Fn type III repeat (*25*−*28*). Integrin−Fn interactions are also crucial for Fn fibrillogenesis, and binding to cells may induce

conformational changes in Fn and expose other masked functional domains (*46*). Incorporation of Fn into a matrix and binding of Fn to fibroblasts can be blocked by Fn fragments containing either the Hep I (70 kDa) or the Hep II (30 kDa) domains (*28*, *47*). The Hep I-containing fragment was shown to be 10-fold more inhibitory than the Hep II fragment in these assays. However, a larger Fn fragment (160 kDa) containing Hep II but not Hep I had no such inhibitory effect, again suggesting a cryptic nature of the Hep II functional domain.

Interactions between the Hep I site and heparin may initiate conformational changes in Fn that are important in Fn−cell interactions and Fn fibrillogenesis. Studies are underway to investigate the physical characteristics of heparin−Fn interactions and the resultant conformational changes in intact Fn molecules using atomic force microscopy.

ACKNOWLEDGMENT

We thank Drs. Nils Almqvist, Ashok Parbhu, Arjan Quist, and Rijinder Bhatia for valuable technical advice.

REFERENCES

1. Humphries, M. J., Obara, M., Olden, K., and Yamada, K. M. (1989) *Cancer Invest. 7*, 373−393.
2. Mosher, D. F. (1989) *Fibronectin*, Academic Press, New York.
3. Hynes, R. O. (1990) *Fibronectins*, Springer-Verlag, New York.
4. Pytela, R., Pierschbacher, M. D., and Ruoslahti, E. (1985) *Cell 40*, 191−198.
5. Vogel, B. E., Tarone, G., Giancotti, F. G., Gailit, J., and Ruoslahti, E. (1990) *J. Biol. Chem. 265*, 5934−5937.
6. Mould, A. P., Komoriya, A., Yamada, K. M., and Humphries, M. J. (1991) *J. Biol. Chem. 266*, 3579−3585.
7. Izzard, C. S., Radinsky, R., and Culp, L. A. (1986) *Exp. Cell Res. 165*, 320−336.
8. Woods, A., Couchman, J. R., Johansson, S, and Höök, M. (1986) *EMBO J. 5*, 665−670.
9. Stathakis, N. E., and Mosesson, M. W. (1977) *J. Clin. Invest. 60*, 855−865.
10. Yamada, K. M., Kennedy, D. W., Kimata, K., and Pratt, R. M. (1980) *J. Biol. Chem. 255*, 6055−6063.
11. Bentley, K. L., Klebe, R. J., Hurst, R. E., and Horowitz, P. M. (1985) *J. Biol. Chem. 260*, 7250−7256.
12. Hayashi, M., Schlesinger, D. H., Kennedy, D. W., and Yamada, K. M. (1980) *J. Biol. Chem. 255*, 10017−10020.
13. Vartio, T. (1982) *Eur. J. Biochem. 123*, 223−233.
14. Gold, L. I., Frangione, B., and Pearlstein, E. (1983) *Biochemistry 22*, 4113−4119.
15. Sekiguchi, K., Hakomori, S., Funahashi, M., Matsumoto, I., and Seno, N. (1983) *J. Biol. Chem. 258*, 14359−14365.
16. Skorstengaard, K., Jensen, M. S., Petersen, T. E., and Magnusson, S. (1986) *Eur. J. Biochem. 154*, 15−29.
17. Siri, A., Balza, E., Carnemolla, B., Castellani, P., Borsi, L., and Zardi, L. (1986) *Eur. J. Biochem. 154*, 533−538.
18. Benecky, M. J., Kolvenbach, C. G., Amrani, D. L., and Mosesson, M. W. (1988) *Biochemistry 27*, 7565−7571.
19. Ingham, K. C., Brew, S. A., and Atha, D. H. (1990) *Biochem. J. 272*, 605−611.
20. Barkalow, F. J., and Schwarzbauer, J. E. (1991) *J. Biol. Chem. 266*, 7812−7818.
21. McCarthy, J. B., Hagen, S. T., and Furcht, L. T. (1986) *J. Biol. Chem. 102*, 179−188
22. Haugen, P. K., McCarthy J. B., Roche, K. F., Furcht, L. T., and Letourneau, P. C. (1992) *J. Neurosci. 12*, 2034−2042.
23. Dalton, B. A., McFarland, C. D., Underwood, P. A., and Steele, J. G. (1995) *J. Cell Sci. 108*, 2083−2092.
24. Mohri, H., Tanabe, J., Katoh, K., and Okubo, T. (1996) *J. Biol. Chem. 271*, 15724−15728.
25. Hocking, D. C., Sottile, J., and McKeown-Longo, P. J. (1994) *J. Biol. Chem. 269*, 19183−19187.
26. Hocking, D. C., Sottile, J., and McKeown-Longo, P. J. (1998) *J. Cell Biol. 141*, 241−253.
27. Aguirre, K. M., McCormick, R. J., and Schwarzbauer, J. E. (1994) *J. Biol. Chem. 269*, 27863−27868.
28. Bultmann, H., Santas, A. J., and Peters, D. M. (1998) *J. Biol. Chem. 273*, 2601−2609.
29. Busby, T. F., Argraves, W. S., Brew, S. A., Pechik, I., Gilliland, G. L., and Ingham, K. C. (1995) *J. Biol. Chem. 270*, 18558−18562.
30. Kishore, R., Samuel, M., Khan, M. Y., Hand, J., Frenz, D. A., and Newman, S. A. (1997) *J. Biol. Chem. 272*, 17078−17085.
31. Fukai, F., Hasebe, S., Ueki, M., Mutoh, M., Ohgi, C., Takahashi, H., Takeda, K., and Katayama, T. (1997) *J. Biochem. 121*, 189−192.
32. Lal, R., and John, S. A. (1994) *Am. J. Physiol. 266*, C1−21.
33. Moy, V. T., Florin, E. L., and Gaub, H. E. (1994) *Science 266*, 257−259.
34. Hinterdorfer, P., Baumgartner, W., Gruber, H. J., Schilcher, K., and Schindler, H. (1996) *Proc. Natl. Acad. Sci. U.S.A. 93*, 3477−3481.
35. Wolberg, A. S., Stafford, D. W., and Erie, D. A. (1997) *J. Biol. Chem. 272*, 16717−16720.
36. Lin, H., Clegg, D. O., and Lal, R. (1999) *Biochemistry 38*, 9956−9963.
37. Erickson, H. P., Carrell, N., and McDonagh, J. (1981) *J. Cell Biol. 91*, 673−678.
38. Engel, J., Odermatt, E., Engel, A., Madri, J. A., Furthmayr, H., Rohde, H., and Timpl, R. (1981) *J. Mol. Biol. 150*, 97−120.
39. Vesenka, J., Manne, S., Yang, G., Bustamante, C. J., and Henderson, E. (1993) *Scanning Microscosc. 7*, 781−788.
40. Cleveland, J. P., Anczykowski, B., Schmid, A. E., and Elings, V. B. (1998) *Appl. Phys. Lett. 72*, 2613−2615.
41. Erickson, H. P., and Carrell, N. A. (1983) *J. Biol. Chem. 258*, 14539−14544.
42. Odermatt, E., Engle, J., Richter, H., and Hörmann, H. (1982) *J. Mol. Biol. 159*, 109−123.
43. Beck, K., Hunter, I., and Engel, J. (1990) *FASEB J. 4*, 148−60.
44. Mosher, D. F., Sottile, J., Wu, C., and McDonald, J. A. (1992) *Curr. Opin. Cell Biol. 4*, 810−818.
45. Schwartz, M. A., Schaller, M. D., and Ginsberg, M. H. (1995) *Annu. Rev. Cell Dev. Biol. 11*, 549−599.
46. Wu, C., Keivens, V. M., O'Toole, T. E., McDonald, J. A., and Ginsberg, M. H. (1995) *Cell 83*, 715−724.
47. McKeown-Longo, P. J., and Mosher, D. F. (1985) *J. Cell Biol. 100*, 364−374.

BI991624O